

79-12-105
高工研圖書室

EUROPEAN ORGANIZATION FOR NUCLEAR RESEARCH

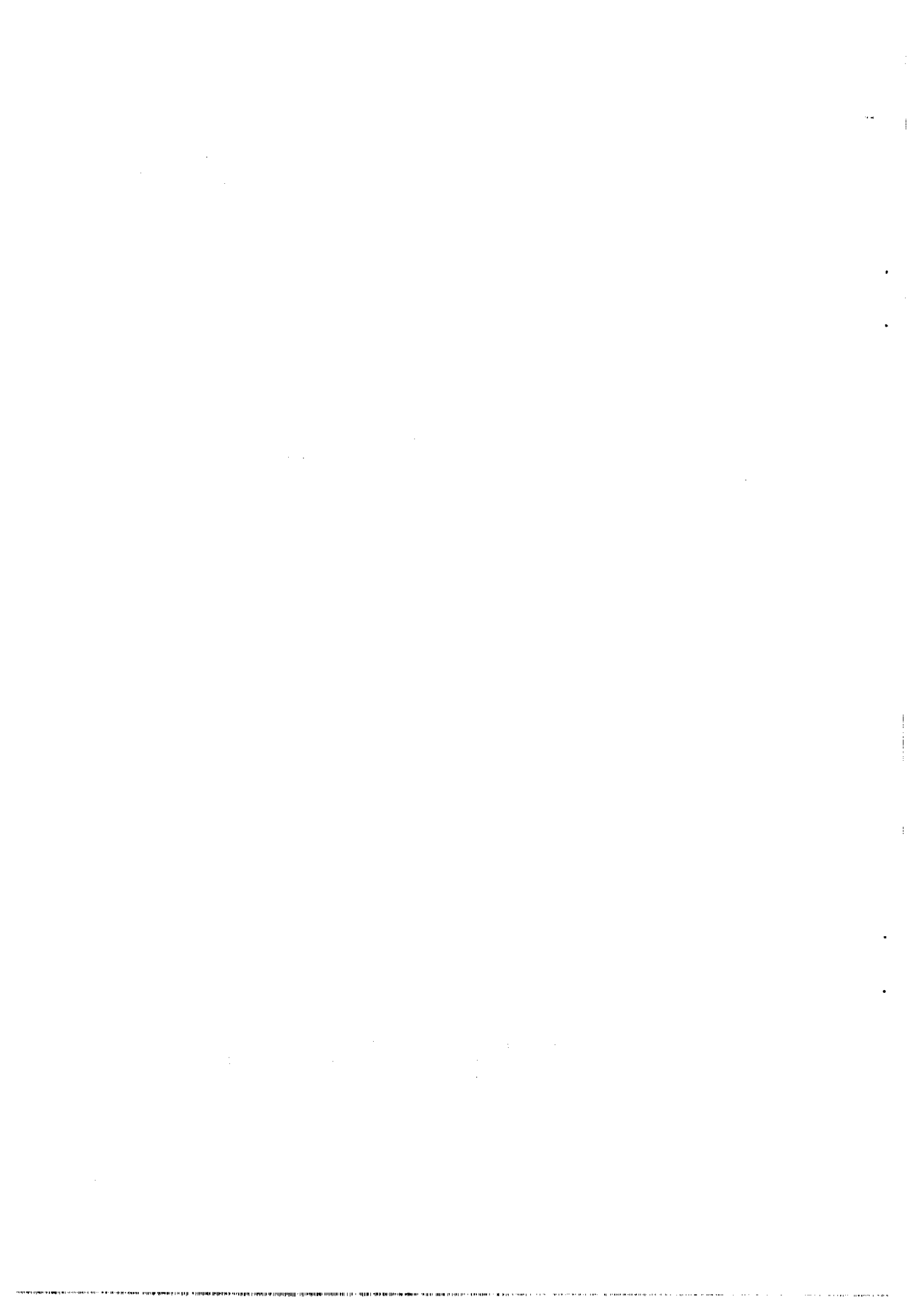
CERN-EP/79-116
4 October 1979

DIMUON SPECTRA FROM 62 GeV PROTON COLLISIONS

CERN-Harvard-Frascati-MIT-Naples-Pisa Collaboration

(presented by U. Becker)

Paper presented at the
EPS International Conference on High-Energy Physics
Geneva, 27 June-4 July 1979



DIMUON SPECTRA FROM 62 GeV PROTON COLLISIONS

CERN-Harvard-Frascati-MIT-Naples-Pisa Collaboration

D. Antreasyan, W. Atwood, V. Balakin, R. Battiston, U. Becker, G. Bellettini, P.L. Braccini, J.G. Branson, J. Burger, F. Carbonara, R. Carrara, R. Castaldi, V. Cavalanni, F. Cervelli, M. Chen, G. Chiefari, T. Del Prete, E. Drago, M. Fujisaki, M. Hodous, T. Lagerlund, P. Laurelli, O. Leistam, R. Little, P.D. Luckey, M.M. Massai, T. Matsuda, L. Merola, M. Morganti, M. Napolitano, H. Newman, D. Novikoff, L. Perasso, K. Reibel, J.P. Revol, R. Rinzivillo, G. Sanguinetti, C. Sciacca, P. Spillantini, K. Strauch, S. Sugimoto, S.C.C. Ting, W. Toki, M. Valdata-Nappi, C. Vannini, F. Vannucci, F. Visco and S.L. Wu

(Presented by U. Becker)

ABSTRACT

Results from an experiment studying $pp \rightarrow \mu^+ \mu^- X$ at the ISR with the highest possible energy of $\sqrt{s} = 62$ GeV are presented. With relatively high statistics at these energies, the measurements extend to very high muon-pair masses. Associated hadron multiplicities are observed.

The continuum of the pair spectra exhibits scaling. The data allow the extraction of the explicit dependence on x_{Feyn} , the transverse momentum p_T , and the decay angle θ . The angular distribution is flat at the T, and $1 + \cos^2 \theta$ otherwise. J and T are seen and measured, as well as very high mass events. Limits of resonance production are estimated.

Here we present data from experiment R209 ¹⁾ measuring

$$pp \rightarrow \mu^+ \mu^- X, \quad (1)$$

which was carried out at the CERN Intersecting Storage Rings (ISR) from the beginning of 1978 to March 1979, with $\sqrt{s} = 62$ GeV and an integrated luminosity of 1.06×10^{38} cm⁻². Observing 11,000 muon pairs with invariant mass above 2.8 GeV, these data provide the best statistical measurement in the range of high masses.

The experiment was designed to study heavy photons in $pp \rightarrow \gamma_V X$, with $\gamma_V \rightarrow \mu^+ \mu^-$, by measuring the pair mass spectrum from 3-20 GeV and the angular distribution together with the multiplicities of the residual hadrons X.

The second aim was to search for new resonances Z, decaying into muon pairs $Z \rightarrow \mu^+ \mu^-$. For this the detector was designed to accept very high pair masses. It also required the highest possible energy -- as available only on the CERN ISR.

1. THE DETECTOR

The detector is shown in Fig. 1a. Seven toroids of magnetized iron surround the interaction region. Muons are identified by penetration, requiring a minimum of 1.8 GeV/c momentum. Hadrons are absorbed in 450 tons of material with 8-11 absorption lengths along the path.

Made from low-carbon steel of the Carnegie-Mellon cyclotron, the rectangular yokes 1a,b,c, 2a,b, and the round ones 3 and 4, are excited by toroidal coils to a rather uniform magnetic field of 1.75 T. This was measured by Hall probes to < 3%, and also independently confirmed by pick-up coils around the yokes.

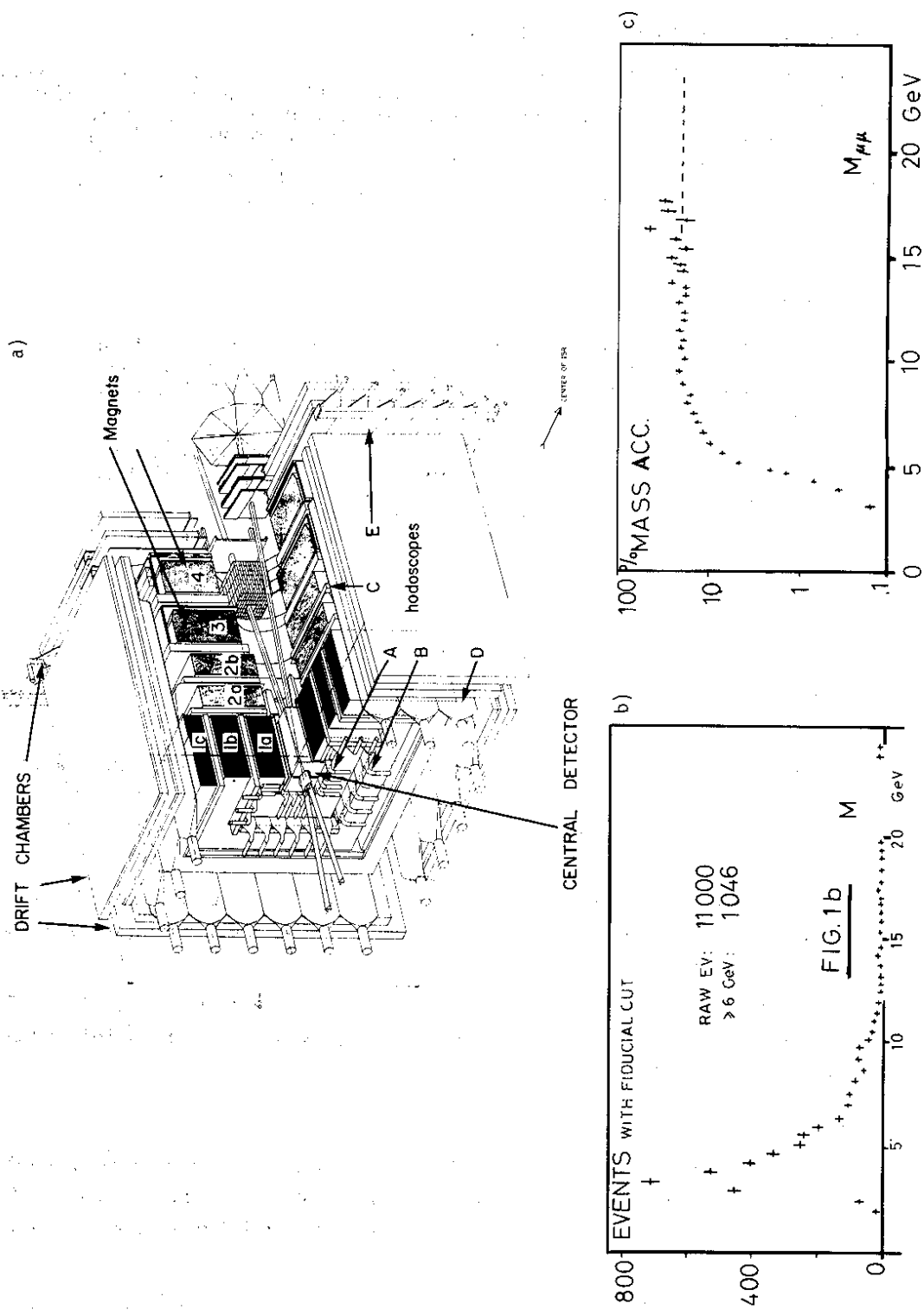


Fig. 1 a) Detector with one quadrant removed for clarity. Shaded areas are the toroidal magnets cut orthogonal to the field lines. b) Event distribution versus reconstructed mass. c) Mass acceptance versus computer-generated mass.

Large-size drift chambers between the magnets and around the detector determine the muon momenta. These chambers have dimensions of up to $6.5 \times 2.7 \text{ m}^2$, and a total of 5000 wires spaced by 101.6 mm. With four planes per chamber²⁾ measuring x,y twice, the left-right ambiguity is resolved and the angle of incidence determined. All the chambers were tested extensively and the resolution was found to be 430 μm . After installation and survey, cosmic rays were used to check their final position with small calibration chambers. Covering $\sim 800 \text{ m}^2$, they contain 60 m^3 of argon + isobutane (75:25% vol. mixture), supplied from a 95% recycling and purifying system.

Immediately around the intersection, an array of 136 precision drift chambers with 544 wires and 272 delay lines indicates all outgoing tracks by 3-5 points, accurate to 0.7 mm along the beam and 3 mm transverse to it. The muon tracks are observed and, together with the hadron tracks, a vertex is determined. The multiplicity and directions of the associated hadrons are measured. An additional system of 34 drift chambers, with 361 wires and 187 delay lines, measure tracks at an angle of 30° down to 1° to the proton beams.

Hodoscopes A, B, C, D, and E form the pair trigger to read out the chambers; their times are precisely recorded on 160 TDCs. Covering 200 m^2 , special precautions were necessary to suppress environmental background. Hodoscope D, with elements of $0.83 \times 4.0 \text{ m}^2$, has fast 5-inch tubes at both ends. The time difference determines the muon position to 25 cm, which can be checked against the chambers; this eliminates multitrack background and accidentals. In addition, fast "mean timers" give position-independent signals which enable the rejection of cosmic rays, these signals being 15 ns out of time. The toroids have a roughly circular field; bending affects the polar angle θ but not the azimuthal angle ϕ (around the beam). The B, C, D, (E) hodoscopes form 24 (48) equal ϕ sectors. Even the worst (3σ) multiple scattering is confined to one sector. Therefore matching combinations (BD, etc.) are formed, allowing also the adjacent elements to define a coarse μ track in the logic. Two tracks at $180^\circ \pm 50^\circ$ yield a trigger.

In summary, the detector has a large acceptance

$$15^\circ < \theta < 130^\circ, \quad p_\mu > 1.8 \text{ GeV}.$$

The π and K decays are small, because the absorber already starts at 40 cm from the vertex.

Figure 1c shows the resulting mass acceptance obtained from a Monte Carlo calculation accounting for multiple scattering energy loss, chamber efficiency, and fiducial cuts as applied to real events. The production mechanism used is consistent with our data.

The momentum resolution is limited by the multiple scattering in iron rather than by the chamber accuracy. One expects $\Delta m/m = 11\%$ almost independent of mass.

2. DATA AND CHECKS

The raw events observed with this apparatus in a year, with $\int L dt = 1.06 \times 10^{38} \text{ cm}^{-2}$, are more than any other measurement in this energy range and are presented in Fig. 1b. To safeguard against systematic errors, half of the data were taken at each magnet polarity. All time and pulse-height recording equipment was frequently recalibrated and compared to pulser signals. The gas composition was tightly controlled by a chromatograph to avoid efficiency fluctuations.

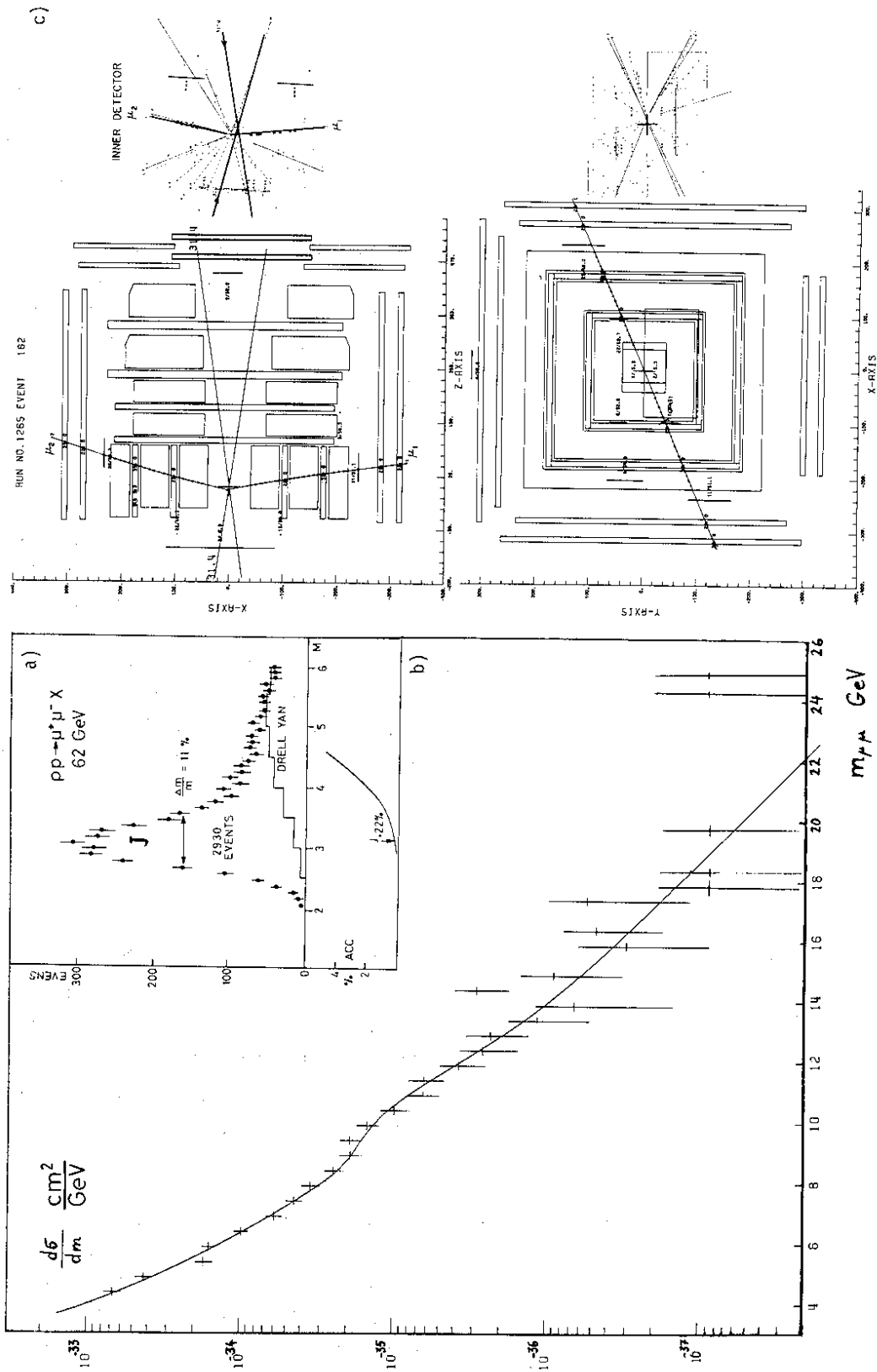


Fig. 2 a) Events in the J region, showing the mass resolution and Drell-Yan contribution. Lower: mass acceptance vs. generated mass. b) Cross-section with simultaneous fit for continuum and $\Upsilon + \Upsilon' + \Upsilon''$ contributions (see text). c) Computer-reconstructed picture of a high mass event. Top view and front view of the detector, accompanied by enlarged view of the tracks in the hadron detector. $M = 24.9 \text{ GeV}$, $p_T = 1.2 \text{ GeV}$, and $x_F = 0.2$.

All events were required to originate from the interaction diamond, as "seen" by the inner detector.

Recording cosmic-ray data with magnetic field and comparing the independently fitted momenta of the upper and lower half of the detector yielded $\Delta p/p \approx 16\%$ as expected, confirming the recognition program. From this the mass resolution is estimated to be $\Delta m/m \approx 16\%/ \sqrt{2}$, almost independent of mass. A very direct check is given by observing the J with an apparent width of 780 MeV as in Fig. 2a, in good agreement with the expected 11% mass resolution.

3. J AND T RESONANCES

Kinematically, the muons from J's produced at rest have 1.55 GeV/c momentum and cannot penetrate the iron (1.8-2 GeV). Instead, we measure J's produced forward with $x_F = p_L/p_{L_{\max}} \approx 0.2$. In this case the decay muons have $p > 2.8$ GeV/c. The acceptance is very small and difficult to calculate, and is accounted for by the conservative errors of the cross-section

$$B_{\mu\mu} \left. \frac{d\sigma}{dy} \right|_0 (J) = \begin{pmatrix} 1^{+1.0} \\ -0.5 \end{pmatrix} \times 10^{-32} \text{ cm}^2 .$$

Figure 2b shows the mass spectrum from 4 to 26 GeV, obtained from the events of Fig. 1b and the acceptance incorporating a $(1-x)^3$ dependence in the Feynman variable x_F , $\exp(-1.0 p_T)$ for transverse momentum, and $(1 + \cos^2 \theta_{\mu^+}^{\text{CS}})$ for angular distribution. All dependences are verified by our data and shown later. The sensitivity to the p_T and x dependence is small, since the detector covers almost the full range. However, taking a flat angular distribution instead of $1 + \cos^2 \theta$ increases the acceptance by 20%. The ansatz

$$\begin{aligned} \frac{d\sigma}{dm} = A \frac{[1 - (m/\sqrt{s})]^{1.0}}{m^4/\sqrt{s}} + B \left\{ \exp \left[- \frac{(1 - 9.4/m)^2}{2\sigma^2} \right] + 0.3 \exp \left[- \frac{(1 - 10/m)^2}{2\sigma^2} \right] \right. \\ \left. + 0.15 \exp \left[- \frac{(1 - 10.4/m)^2}{2\sigma^2} \right] \right\} \end{aligned}$$

with $\sigma = 10\%$ was fitted to the data of Fig. 2b. With $\chi^2/DF = 17.2/21$, we obtain

$$B_{\mu\mu} \cdot \sigma(\tau) = 10 \pm 3.5 \text{ pb}$$

using a flat angular distribution. The result for the continuum can be recast into the familiar scaling form³⁾:

$$m^3 \frac{d\sigma}{dm} = (7.7 \pm 0.4) \times 10^{-33} (1 - \sqrt{\tau})^{1.0} / \sqrt{\tau} \text{ GeV}^2 \text{ cm}^2$$

with $\tau = m^2/s$. In addition to the quoted errors, the over-all normalization has an uncertainty of 40%.

4. HIGH-MASS EVENTS

As seen in Fig. 2b, both the data and the scaling prediction decrease to less than $2 \times 10^{-37} \text{ cm}^2$ above 20 GeV mass. However, after a gap of several GeV there are two more events at ~ 25 GeV (and one not shown from older data at 28 GeV). The computer-reconstructed picture of one event at 24.9 GeV is shown in Fig. 2c. The front view gives the event in the non-bending plane. Each track has complete sets of coordinates linking to the tracks of the inner detector shown at the right-hand side. The counters initiating the trigger are all within 1.6 ns. The top view displays the excellent momentum fit. The tracks form an angle, seen also in the hadron detector, and with the time information this clearly excludes a cosmic ray. Together with 12 more charged hadrons they emerge from a point well within the interaction diamond. Also indicated is the position using the time difference of both phototubes at the D hodoscope. This matches nicely with the tracks observed with chambers. The event is clean, i.e. does not contain spurious chamber coordinates. This feature is quite common to all events, demonstrating the effectiveness of the iron shielding.

5. ASSOCIATED HADRONS

The hadron detector allows the multiplicity and directions of charged hadrons to be determined. Momenta are not measured. Looking at the track distribution with respect to one of the muons, no correlation was observed. As a function of the dimuon energy $E_{\mu\mu}$ the total multiplicity decreases consistently with the multiplicity expected at the lower energy of $\sqrt{s} - E_{\mu\mu}$.

The multiplicity increases with p_T of the muon pair. Interestingly, this increase happens exclusively in the hemisphere opposing the transverse momentum of the μ pair (see Fig. 3a).

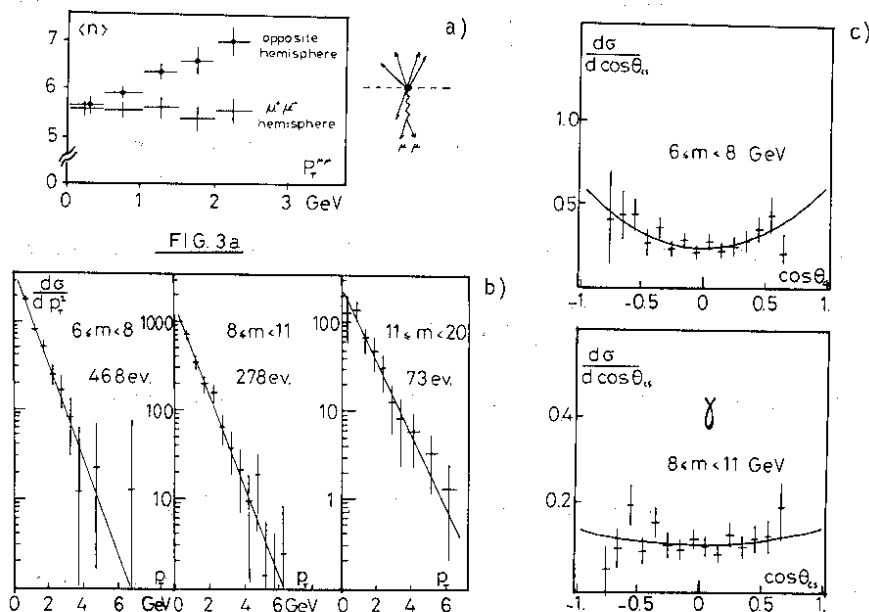


Fig. 3 a) Charged-track multiplicity in the hemisphere of the μ pair. Notice the rise in the opposite one. b) p_T dependence of the dimuons in the 6-8 GeV, the 8 GeV, and the hitherto unexplored 11-20 GeV regions. c) Collins-Soper angular distribution of μ^+ .

6. x_F AND p_T DEPENDENCE

Above $m = 6$ GeV the acceptance is reasonably flat. Comparing the cross-section measured in $-0.1 < x_F < 0.7$ with the form

$$(1 - |x|)^A$$

we find for

$$468 \text{ events in } 6 < m < 8 \text{ GeV}, \quad A = 3.0 \pm 0.3$$

and

$$278 \text{ events in } 8 < m < 11 \text{ GeV}, \quad A = 3.2 \pm 0.3.$$

For the same intervals and, additionally, for $11 < m < 20$ GeV the cross-sections $(1/p_T)(d\sigma/dp_T)$ are shown in Fig. 3b in relative units. Neglecting the first (low) bin, a good fit to $\exp(-bp_T)$ can be obtained with the result:

$$b = 1.20 \pm 0.11 \quad 1.18 \pm 0.10 \quad 0.97 \pm 0.17 \text{ GeV}^{-1}$$

for

$$m = \quad 6-8 \quad \quad \quad 8-11 \quad \quad \quad 11-20 \quad \text{GeV}.$$

No difference for the 8-11 region containing the T is seen when this is compared with the other regions. This observation and the measured shape are in good agreement with recent calculations⁴⁾.

7. AVERAGE TRANSVERSE MOMENTUM $\langle p_T \rangle$

Three different complementary methods were used to determine $\langle p_T \rangle$:

- a) from $d\sigma/dp_T^2 \sim e^{-bp_T}$ there follows: $\langle p_T \rangle = 2/b$;
- b) directly (correcting for acceptance): $\langle p_T \rangle = (1/N) \sum_{i=1}^N p_T^i$;
- c) change e^{-bp_T} in the Monte Carlo generation until the best match to the observed event distribution is obtained. This ensures best treatment of the resolution.

The results are summarized in Table 1 for three ranges of dimuon mass.

Table 1

Average transverse momentum in GeV/c

Mass range	6-8	8-11	11-20
a)	1.60 ± 0.15	1.70 ± 0.17	$2.0^{+0.5}_{-0.25}$
b)	1.68 ± 0.19	1.77 ± 0.10	2.0 ± 0.20
c)	1.8 ± 0.2	1.7 ± 0.26	2.1 ± 0.4

These values are definitely higher than those observed at FNAL³⁾, at the same mass but with $\sqrt{s} = 27.4$ GeV, and suggest a substantial \sqrt{s} dependence.

8. DECAY ANGULAR DISTRIBUTION

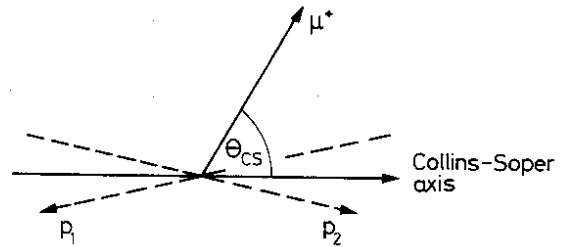
Crucial to the Drell-Yan picture of parton antiparton annihilation are the predictions of

- i) SCALING: $m^3 \frac{d\sigma}{dm} = F\left(\tau = \frac{m^2}{s}\right)$, and
- ii) angular distribution

$$\frac{d\sigma}{d\Omega} \sim 1 + \cos^2 \theta_{\mu^+}$$

following from the spin $\frac{1}{2}$ constituents.

However, the original model ignores p_T . Choosing the reference axis z of Collins and Soper⁵⁾ which averages the proton directions p_1, p_2 , as seen from the μ -pair c.m.s., one should see to leading order the $1 + \cos^2 \theta_{CS}$ distribution. Figure 3c supports this for



$$6 < m < 8 \text{ GeV} \quad \text{with} \quad 1 + (1.6 \pm 0.7) \cos^2 \theta_{CS} .$$

However it is remarkably less pronounced and consistent with being flat in the τ region:

$$8 < m < 11 \text{ GeV} \quad \text{with} \quad 1 + (0.3 \pm 0.6) \cos^2 \theta_{CS} ,$$

suggesting another production mechanism. With $\chi^2/DF = 8.2/12$ and $11/12$ these are reasonable fits. The data were integrated over all $x < 0.7$.

9. MULTIMUONS

In order to penetrate the iron of the detector, muons must have $p > 1.8$ - 2.2 GeV depending on the geometry. The geometrical angular acceptance for each muon is 0.4. Trigger constraints will reduce trimuons by 0.5. Six trimuon events were observed with an integrated luminosity of $1.06 \times 10^{38} \text{ cm}^{-2}$. Two of these events clearly involved a vector-meson mass (J) in one $\mu^+ \mu^-$ combination and a third track of bad quality. The remaining four events can be used to pose an upper 2σ limit

$$\sigma(3\mu) < \frac{8 \text{ events} \times 10^{38}}{0.5 \times 0.4^3 \times 1.06} = 2.4 \text{ pb} ,$$

for $pp \rightarrow 3\mu + X$ with $p_\mu > 2$ GeV, which includes channels such as $B\bar{B}$ production with subsequent cascade decays⁶⁾ into muons.

10. CONCLUSION

Measuring $pp \rightarrow \mu\mu X$ at $\sqrt{s} = 62$ GeV we find:

$$B \frac{d\sigma}{dy}_0(J) = \left(1 \begin{matrix} + 1 \\ - 0.5 \end{matrix} \right) \times 10^{-32} \text{ cm}^2 ,$$

$$B\sigma(\tau) = 10 \pm 3.5 \text{ pb} .$$

Three high-mass events with $m > 24$ GeV enable a 2σ upper limit to be set on resonance production above 20 GeV:

$$B\sigma < \frac{3 + 2\sqrt{3}}{\text{Acc} \cdot L} = 40 \times 10^{-38} \text{ cm}^2 ,$$

where $\text{Acc} = 0.15$ is the acceptance and $L = 1.06 \times 10^{38} \text{ cm}^{-2}$ is the luminosity. The continuum is measured to small values of τ and is compatible with scaling³⁾:

$$m^3 \frac{d\sigma}{dm} = (7.7 \pm 0.4) \times 10^{-33} (1 - \sqrt{\tau})^{10} / \sqrt{\tau} \text{ GeV}^2 \text{ cm}^2 .$$

The associated hadron multiplicity diminishes with $E_{\mu\mu}$ but increases with p_T in the opposite hemisphere.

The $(1 + \cos^2 \theta_{CS})$ distribution is seen, but not at the T, and $\langle p_T \rangle \approx 1.8 \pm 0.2$ GeV is markedly higher than the values measured at lower \sqrt{s} .

Acknowledgement

It is a pleasure to thank CERN and particularly the ISR groups for continuous support.

REFERENCES

- 1) G. Diambri-Palazzi, U. Becker, P.J. Biggs, G. Everhard, R. Little, K. Strauch and S.C.C. Ting, Proposal CERN/ISR 73-28 (1973) and Colloquium talk by S.C.C. Ting at CERN, December 1978.
- 2) U. Becker, J.D. Burger, D. Novikoff and L. Perasso, Nucl. Instrum. Methods 128, 593 (1975).
- 3) K. Kinoshita, H. Satz and D. Schildknecht, Phys. Rev. D 17, 1834 (1978). The coefficient was determined by fit and agrees with L. Lederman, 19th Int. Conf. on High-Energy Physics, Tokyo, 1978 (Physical Society of Japan, Tokyo, 1979), p. 706.
- 4) Z. Kunszt, E. Pietarinen and E. Reya, DESY preprint 79/28 (1979), submitted to Phys. Lett.
- 5) J.C. Collins and D.E. Soper, Phys. Rev. D 16, 2219 (1977).
- 6) A. Ali, Z. Phys. 1C, 25 (1979).

